

Search for K^+ decays to a lepton and invisible particles

Roberta Volpe ^{*a}

^aFaculty of Mathematics, Physics and Informatics, Comenius University Mlynská dolina F1,
842 48 Bratislava, Slovakia.

Present address: Department of Physics and Geology, Perugia University,
Via Pascoli, 06123, Perugia, Italy

E-mail: roberta.volpe@cern.ch

The NA62 experiment at CERN reports searches for $K^+ \rightarrow e^+N$, $K^+ \rightarrow \mu^+N$ and $K^+ \rightarrow \mu^+X$ decays, where N and X are massive invisible particles, using the 2016-2018 data set. The N particle is assumed to be a heavy neutral lepton, and the results are expressed as upper limits of $O(10^{-9})$ and $O(10^{-8})$ on the neutrino mixing parameter $|U_{e4}|^2$ and $|U_{\mu 4}|^2$, improving on the earlier searches for heavy neutral lepton production and decays in the kinematically accessible mass range. The X particle is considered a scalar or vector hidden sector mediator decaying to an invisible final state, and upper limits of the decay branching fraction for X masses in the range 10-370 MeV/ c^2 are reported for the first time, ranging from $O(10^{-5})$ to $O(10^{-7})$. An upper limit of $1.0 \cdot 10^{-6}$ is established at 90% CL on the $K^+ \rightarrow \mu^+ \nu \bar{\nu}$ branching fraction.

7th Symposium on Prospects in the Physics of Discrete Symmetries (DISCRETE 2020-2021)
29th November - 3rd December 2021
Bergen, Norway

^{*}speaker for the NA62 Collaboration: A. Akmete, R. Aliberti, F. Ambrosino, R. Ammendola, B. Angelucci, A. Antonelli, G. Anzivino, R. Arcidiacono, T. Bache, A. Baeva, D. Baigarashev, L. Bandiera, M. Barbanera, J. Bernhard, A. Biagioni, L. Bician, C. Biino, A. Bizzetti, T. Blazek, B. Bloch-Devaux, P. Boboc, V. Bonaiuto, M. Boretto, M. Bragadireanu, A. Briano Olvera, D. Britton, F. Brizioli, M.B. Brunetti, D. Bryman, F. Bucci, T. Capussella, J. Carmignani, A. Ceccucci, P. Cenci, V. Cerny, C. Cerri, B. Checcucci, A. Conovaloff, P. Cooper, E. Cortina Gil, M. Corvino, F. Costantini, A. Cotta Ramusino, D. Coward, P. Cretaro, G. D'Agostini, J. Dainton, P. Dalpiaz, H. Danielsson, M. D'Errico, N. De Simone, D. Di Filippo, L. Di Lella, N. Doble, B. Dobrich, F. Duval, V. Duk, D. Emelyanov, J. Engelfried, T. Enik, N. Estrada-Tristan, V. Fallaleev, R. Fantechi, V. Fascianelli, L. Federici, S. Fedotov, A. Filippi, R. Fiorenza, M. Fiorini, O. Frezza, J. Fry, J. Fu, A. Fucci, L. Fulton, E. Gamberini, L. Gatignon, G. Georgiev, S. Ghinescu, A. Gianoli, M. Giorgi, S. Giudici, F. Gonnella, K. Gorshanov, E. Goudzovski, C. Graham, R. Guida, E. Gushchin, F. Hahn, H. Heath, J. Henshaw, Z. Hives, E.B. Holzer, T. Husek, O. Hutanu, D. Hutchcroft, L. Iacobuzio, E. Iacopini, E. Imbergamo, B. Jenninger, J. Jerhot, R.W. Jones, K. Kampf, V. Kekelidze, D. Kereibay, S. Kholodenko, G. Khorialui, A. Khotyantsev, A. Kleimenova, A. Korotkova, M. Koval, V. Kozuharov, Z. Kucerova, Y. Kudenko, J. Kunze, V. Kurochka, V. Kurshetsov, G. Lanfranchi, G. Lamanna, E. Lari, G. Latino, P. Laycock, C. Lazzeroni, M. Lenti, G. Lehmann Miotto, E. Leonardi, P. Lichard, L. Litov, P. Lo Chiatto, R. Lollini, D. Lomidze, A. Lonardo, P. Lubrano, M. Lupi, N. Lurkin, D. Madigozhin, I. Mannelli, A. Mapelli, F. Marchetto, R. Marchevski, S. Martellotti, P. Massarotti, K. Massri, E. Maurice, A. Mazzolari, M. Medvedeva, A. Mefodev, E. Menichetti, E. Migliore, E. Minucci, M. Mirra, M. Misheva, N. Molokanova, M. Moulson, S. Movchan, M. Napolitano, I. Neri, F. Newson, A. Norton, M. Noy, T. Numao, V. Obraztsov, A. Okhotnikov, A. Ostankov, S. Padolski, R. Page, V. Palladino, I. Panichi, A. Parenti, C. Parkinson, E. Pedreschi, M. Pepe, M. Perrin-Terrin, L. Peruzzo, P. Petrov, Y. Petrov, F. Petrucci, R. Piandani, M. Piccini, J. Pinzino, I. Polenkevich, L. Pontisso, Yu. Potrebenikov, D. Protopopescu, M. Raggi, M. Reyes Santos, M. Romagnoni, A. Romano, P. Rubin, G. Ruggiero, V. Ryjov, A. Sadovsky, A. Salamon, C. Santoni, G. Saracino, F. Sargeni, S. Schuchmann, V. Semenov, A. Sergi, A. Shaikhiev, S. Shkarovskiy, M. Soldani, D. Soldi, M. Sozzi, T. Spadaro, F. Spinella, A. Sturgess, V. Sugonyaev, J. Swallow, A. Sytov, G. Tinti, A. Tomczak, S. Trilov, M. Turisini, P. Valente, B. Velghe, S. Venditti, P. Vicini, R. Volpe, M. Vormstein, H. Wahl, R. Wanke, V. Wong, B. Wrona, O. Yushchenko, M. Zamkovsky, A. Zinchenko

1. Introduction

The neutrinos are the only fermions of the Standard Model (SM) with only one chirality. Furthermore they are massless in the SM while non-zero masses are measured. Several beyond SM scenarios foresee the existence of right-handed neutrinos, or heavy neutral leptons (HNLs), for example the Neutrino Minimal Standard Model ($\nu MSSM$) [1] assumes three HNLs. The $\nu MSSM$ accounts for dark matter, baryogenesis, neutrino masses and oscillations provided that two HNLs are in the MeV–GeV mass range and a third HNL, a dark matter candidate, at the keV mass scale. In this scenario the production of HNLs in SM decays and the decay of HNLs to SM particles proceed because of a mixing between the SM neutrinos and the HNLs. For small values of the mixing parameter and assuming that HNLs (also called N s in the following) decay only to SM particles, the lifetime of one of such HNLs is so long that it will not decay within NA62, resulting in missing mass. This document reports the results of searches performed by the NA62 experiment in the two channels: $l = e, \mu$. The final state with a muon and nothing else, is also exploited to search for a new particle X , produced in the decay $K^+ \rightarrow \mu\nu X$, and decaying to invisible particles. This search is motivated by a scenario, which explains the muon $g-2$ anomaly and dark matter (DM) freeze-out through a scalar or vector hidden sector mediator X coupling preferentially to the muon [2]. For a mediator with mass $m_X < m_K - m_\mu$ the decay $K^+ \rightarrow \mu\nu X$ would have a branching fraction of $O(10^{-8})$ and be followed by a prompt decay of the mediator with a sizeable invisible branching fraction [3]; indeed in the light DM freeze-out model, X decays to DM particles. Another by-product of the muon channel is the search for the decay $K^+ \rightarrow \mu^+ \nu \nu \bar{\nu}$, which in the SM occurs at second order in the Fermi constant with a BR of $1.62 \cdot 10^{-16}$ and is experimentally out of reach. The strongest upper limit to date is $BR(K^+ \rightarrow \mu^+ \nu \nu \bar{\nu}) < 2.4 \cdot 10^{-6}$ at 90% CL [4].

2. The NA62 experiment and event selection

The NA62 experiment has been designed to measure the branching ratio $\mathcal{B}(K^+ \rightarrow \pi^+ \nu \bar{\nu})$ with high precision, a schematic view is shown in Figure 1 and the details of the beam line and detectors are described in [5]. An overview of the main detectors used in this work is given here. The 400

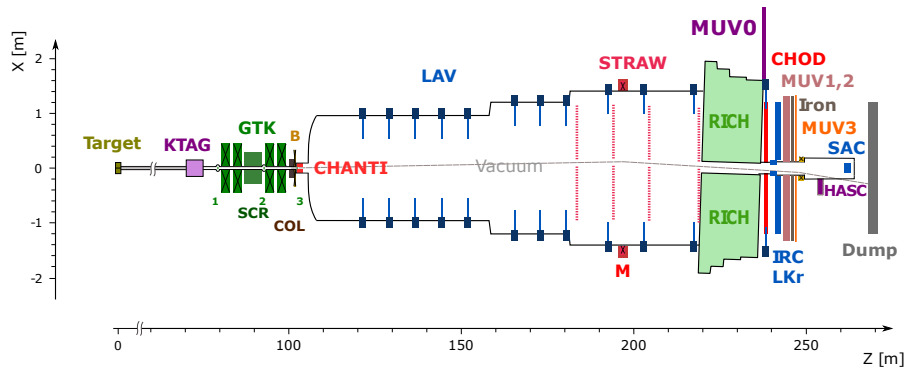


Figure 1: Schematic side view of the NA62 beamline and detector.

GeV/ c proton beam provided by the SPS accelerator impinges on a berillyum target giving rise to a secondary beam of particles of which 6% are kaons with a nominal momentum of 75 GeV/ c . They

are identified by a differential Cherenkov counter (KTAG) with a 70 ps resolution and their momenta are measured by the beam spectrometer (GTK). A magnetic spectrometer (STRAW) measures the momenta and directions of the charged particles produced by the decays of the kaons in a 75 m long fiducial volume (FV). Powerful particle identification (PID) comes from the combination of a Ring Imaging Cherenkov detector (RICH), a liquid krypton calorimeter (LKr), and a muon detector system (MUV). A hermetic photon veto system is composed of the LKr and a twelve ring-shaped lead-glass detectors (LAV). Two charged hodoscopes are located between the RICH and the LKr, and provide trigger signals and time measurement.

The event selection and analysis strategy is detailed in [6] and [7], a brief summary is reported here. The rates of the signal processes are measured with respect to the SM $K^+ \rightarrow l^+ \nu$ decay rate, reducing systematic uncertainties. Candidate signal and normalization decays are characterised by a single charged lepton (a positron or a muon) and no other detectable particles in the final state. The event selection is optimized to suppress the main background contributions, which arise from beam particle decays upstream of the vacuum tank, decays to multiple detectable particles, and inelastic interactions of beam particles with a station of the GTK. The main event selection requires a single positively charged track reconstructed in the STRAW spectrometer, in the geometrical acceptance of the LKr, CHOD, and MUV3 detector, and identified as a lepton by the PID detectors. Positron and muons are separated with additional requirements. Positrons are required to have momentum p between 5 GeV/c and 30 GeV/c, the ratio between the energy deposited in the LKr (E) and p (E/p) must be in the range 0.92-1.08, and there should be no hits in the muon detector consistent in space and time with the reconstructed track. Muons are required to have momenta between 5 GeV/c and 70 GeV/c, $E/p < 0.2$, and a hit in the muon detector consistent in space and time with the reconstructed track. For tracks with $p < 30$ GeV/c, a RICH-based particle identification algorithm was also applied to distinguish between positrons and muons. Time matching between the KTAG signal and the lepton detection reduces the contribution from beam pions. The K^+ track reconstructed in the GTK is matched with the lepton track using a discriminant based on the time difference and the closest distance of approach. Backgrounds from multi-body K^+ decays are suppressed by veto conditions imposed on other tracks reconstructed by the STRAW spectrometer, additional energy deposits in the LKr, energy deposits in the photon veto system, and additional signals in the CHOD. Pile-up background resulting from kaon decay in the beam line is reduced by applying geometrical constraints on the longitudinal position of the reconstructed vertex. The main discriminant variable is the missing mass squared $m_{miss}^2 = (P_K - P_l)^2$. Figure 2 shows the distribution of data and MC simulation events after the selection in m_{miss}^2 for the e^+ and μ^+ channels. The peak at $m_{miss}^2 = 0$ for the SM decays is used to select the normalization samples, requiring $|m_{miss}^2| < 0.01$ GeV²/c⁴. The m_{miss}^2 distribution for the e channel exhibits a sharp increase around $|m_{miss}^2| = 0.13$ GeV²/c⁴, due to background from beam pion decays. This threshold depends on the maximum positron momentum. Therefore, an "auxiliary" selection with lower selection efficiency was defined imposing $p < 20$ GeV.

3. $K^+ \rightarrow l^+ N$ search strategy

The signal decay $K^+ \rightarrow l^+ N$ is characterised by a narrow peak in the reconstructed missing mass m_{miss} spectrum, while the background has a smooth distribution. Counting experiments

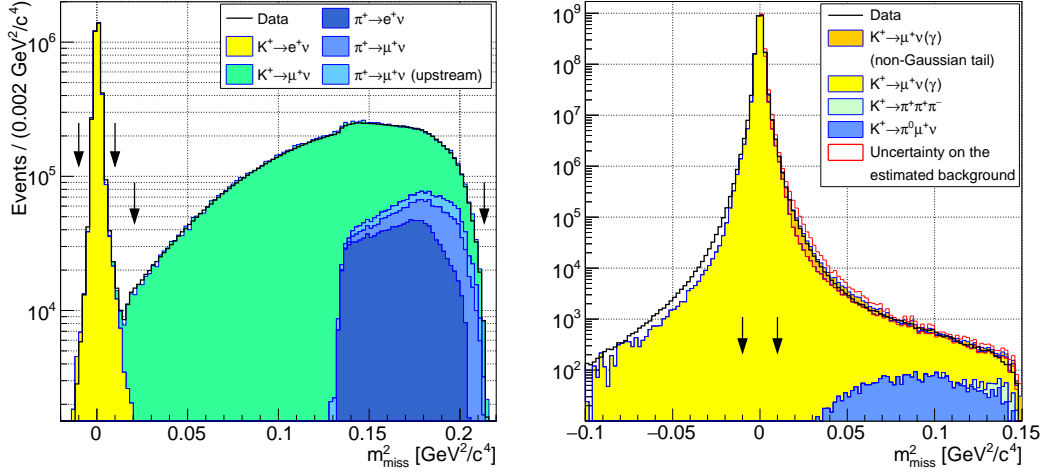


Figure 2: Left (Right): Distribution of m_{miss}^2 for the e^+ (μ^+) channel.

are performed for several mass hypothesis m_N by selecting a window in the m_{miss} distribution $|m_{miss} - m_N| < 1.5\sigma_m$ where σ_m is the m_N resolution evaluated with signal MC. The resolution is strongly dependent on the HNL mass and varies from $\sim 9 \text{ MeV}/c^2$ for $m_N = 50 \text{ MeV}/c^2$ to $\sim 0.5 \text{ MeV}/c^2$ for $m_N = 450 \text{ MeV}/c^2$. The background is evaluated by fitting the sidebands $1.5\sigma_m < |m_{miss} - m_N| < 11.25\sigma_m$ of the data distribution, with a second order polynomial.

Assuming that each SM flavor mixes dominantly with one N , the branching fraction of the decay $K^+ \rightarrow l^+ N$ ($l = e, \mu$) can be expressed as:

$$B(K^+ \rightarrow l^+ N) = B(K^+ \rightarrow l^+ \nu) \cdot \rho_l(m_N) \cdot |U_{l4}|^2 \quad (1)$$

where $B(K^+ \rightarrow l^+ \nu)$ is the measured branching fraction of the SM leptonic decay, $|U_{l4}|^2$ is the mixing parameter, m_N is the HNL mass, and $\rho_l(m_N)$ is a kinematic factor [8], which depends on the N mass and the flavor. The expected number of $K^+ \rightarrow l^+ N$ signal events N_S can be written as

$$N_S = \mathcal{B}(K^+ \rightarrow l^+ N) \cdot N_K \cdot A_N, \quad (2)$$

where A_N is the signal selection acceptance and N_K is the number of selected K decays. The number of kaons N_K is obtained with the normalization selection and is $N_K = (3.52 \pm 0.02) \times 10^{12}$ for the e channel and $N_K = (1.14 \pm 0.02) \times 10^{10}$ for the μ channel. The CLs method [9] is used to obtain the expected and observed upper limit at 90% CL on the number of signal events N_S for each mass hypothesis and each channel. The corresponding upper limits on the mixing parameter $|U_{l4}|^2$ are derived from eq.(2)(1). The resulting observed upper limits are shown in Figure 3 where a full picture of the world best limits is given for the mass range 20-450 MeV/c^2 . In the positron mode this result improves the previous NA62 results by $O(100)$ and in the muon mode it reaches the E949 sensitivity in the 200-300 MeV/c^2 range and extends the constraint on HNL masses up to 384 MeV/c^2 .

4. Searches for $K^+ \rightarrow \mu^+ \nu X$ and $K^+ \rightarrow \mu \nu \nu \bar{\nu}$

The processes $K^+ \rightarrow \mu^+ \nu X$ and $K^+ \rightarrow \mu \nu \nu \bar{\nu}$ are not two-body decays, therefore their spectra in m_{miss}^2 are broad distributions as shown in Figure 4(left). The presence of these signal decays would

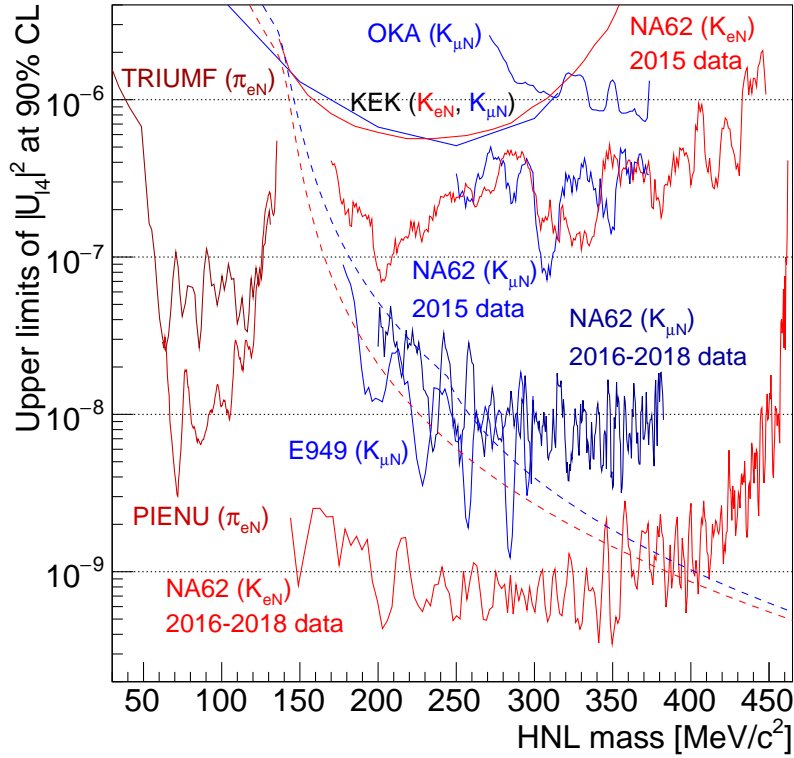


Figure 3: Full picture of the global observed upper limits at 90% CL for the mixing parameter $|U_{l4}|^2$ in the νSMS model. The lower boundaries imposed by the BBN constraint are shown by the dashed lines [10]. Red (blue) dashed line refers to e (μ) channel.

manifest itself with an excess of events over the background. In this case the background evaluation from sideband data is not appropriate and its estimation relies on the MC simulation after a data driven correction is applied. With the assumption that the non-Gaussian tails of the m_{miss}^2 spectrum are left-right symmetrical (see Figure 2), a *tail* component is added to the estimated background in each m_{miss}^2 bin in the region $m_{miss}^2 > 0$ equal to the difference between the data and simulated spectra in the symmetric mass bin with respect to $m_{miss}^2 = 0$. A 100% uncertainty is conservatively assigned to this component to account for the above assumption. The search is performed in a region $m_{miss}^2 > m_0^2$ where m_0^2 is optimized to extract the strongest limits for $K^+ \rightarrow \mu\nu\nu\bar{\nu}$ and each mass hypothesis of $K^+ \rightarrow \mu^+\nu X$. Upper limits at 90% CL on $BR(K^+ \rightarrow \mu^+\nu X)$ are obtained with the CLs method and are shown in Fig.4(right) for 37 mass hypotheses, in the scalar and vector X models. The limits obtained in the scalar model are stronger than those in the vector model due to the larger mean m_{miss} value. In the search for the $K^+ \rightarrow \mu\nu\nu\bar{\nu}$ decay, with $m_0^2 = 0.1 \text{ GeV}^2/c^4$ the number of observed events is $N_{obs} = 6894$ and the number of expected background events is $N_{exp} = 7549 \pm 928$. The resulting observed upper limit on $B(K^+ \rightarrow \mu\nu\nu\bar{\nu})$ is 1.0×10^{-6} at 90% CL.

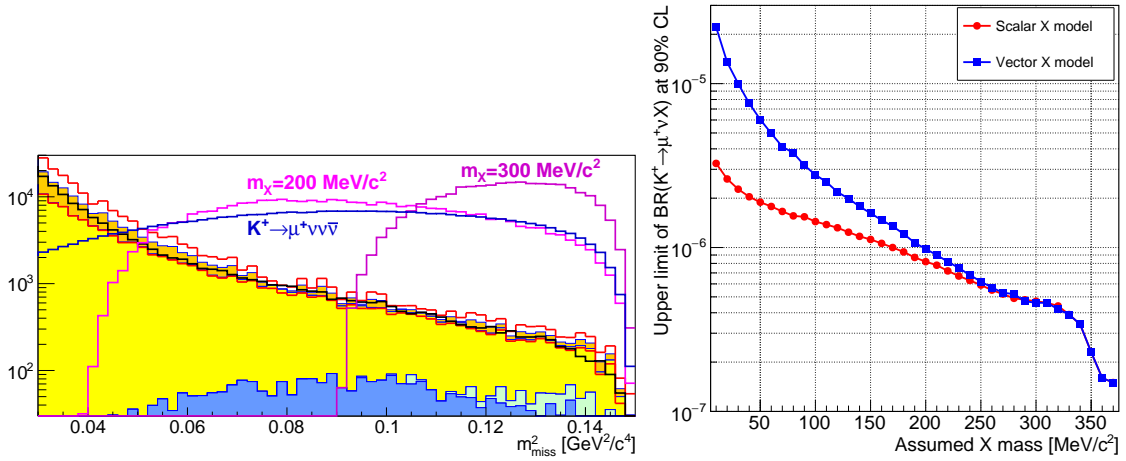


Figure 4: Left: m_{miss}^2 distribution for data, background simulation with correction and for the signals: $K^+ \rightarrow \mu \nu \nu \bar{\nu}$ and $K^+ \rightarrow \mu^+ \nu X$ for two values of m_X . Right: Observed upper limit on $BR(K^+ \rightarrow \mu^+ \nu X)$ as a function of m_X , assuming a scalar (red points) or vector (blue points) X mediator.

5. Summary

The NA62 experiment exploited its capability to select events with a single track to release world-leading results in the search for hidden sector searches. In this document the search for final states with a charged lepton and nothing else is interpreted in different new physics scenarios. In the νMSM scenario, the two-body decay searches give the world best upper limit in the mass range 144-462 MeV/c^2 for the positron channel and in the mass range 300-384 MeV/c^2 for the muon channel. Upper limits on $B(K^+ \rightarrow \mu^+ \nu X)$, where X is either a scalar or vector boson with mass in the range 10-370 MeV/c^2 that decays to DM particles, were set for the first time. Finally, the upper limit on $B(K^+ \rightarrow \mu \nu \nu \bar{\nu})$ was improved.

References

- [1] T. Asaka, M. Shaposhnikov, Phys. Lett. B 620 (2005) 17.
- [2] S.N. Gninenko, N.V. Krasnikov, Phys. Lett. B 513 (2001) 119.
- [3] G. Krnjaic, et al., Phys. Rev. Lett. 124 (2020) 041802.
- [4] A.V. Artamonov, et al., Phys. Rev. D 94 (2016) 032012.
- [5] E. Cortina Gil et al., J. Instrum. 12, P05025 (2017).
- [6] E. Cortina Gil et al., Phys. Lett. B 807 (2020) 135599.
- [7] E. Cortina Gil et al., Phys. Lett. B 816 (2021) 136259.
- [8] R. Shrock, Phys. Lett. B 96 (1980) 159; Phys. Rev. D 24 (1981) 1232.
- [9] A.L. Read, J. Phys. G 28 (2002) 2693.
- [10] A.D. Dolgov et al. Nuclear Physics B 590 (2000).